Final report: Understanding ashfall hazards from a future eruption at Taupo caldera (EQC project 16/724)

Principal Investigator: *Dr Simon Barker (University of Auckland)*

Research team
Prof. Shane Cronin, Dr Mary Anne Thompson (University of Auckland)
Dr Alexa Van Eaton, Dr Larry Mastin (United States Geological Survey)
Dr Thomas Wilson (University of Canterbury)
Prof. Colin Wilson (Victoria University of Wellington)
Dr Cory Davis (MetService, Wellington)

Key words: *Volcano, Taupo volcano, Volcanic ash, hazard, volcanic eruption, caldera, supereruption, risk, vulnerability, weather, numerical modelling*

Summary

Hazard analysis at caldera volcanoes is challenging because of the wide range of potential eruptive sizes and conditions that can plausibly occur in any single event. Ashfall hazards can impact huge areas, with even small amounts of volcanic ash causing widespread damage, disruption and economic costs. Taupo volcano in the central North Island is one of the most frequently active and productive caldera volcanoes on Earth and host to the youngest known supereruption ~25,400 years ago. Over the past 12,000 years there have been at least 25 more eruptions from Taupo that span 3-4 orders of magnitude in size and recent studies suggest that there is still a large magma system that could generate another eruption on timescales of human concern. In this EQC-funded project we have combined our current understanding of Taupo's eruptive record with one of the most advanced ash dispersal models; Ash3d, to build a better understanding of which areas of New Zealand would experience ashfall across a range of eruption sizes and wind conditions. For the smallest eruptions considered (~0.1 km^3 magma), ashfall to >1 cm thickness is largely confined to the central North Island and dispersal is dictated mostly by day-to-day weather. Only major population centres in the eastern North Island between Tauranga and Hastings can expect >1 mm ashfall with probabilities between 10 and 30%. However, with increasing eruption sizes (1-5 km^3 magma), the probability of ash thickness to reach damaging levels (10-100 mm) becomes increasingly significant, especially in the Gisborne, Hawke's Bay, Bay of Plenty, Waikato and Manawatu regions. With increasing eruption size, ash dispersal becomes less dependent on weather, as the formation of a major umbrella cloud may force ash upwind or cross-wind. For the largest eruptions (50-500 km^3), ash thicknesses associated with major damage (100mm) or severe structural damage (>300 mm) can be expected at high probabilities in most major towns or cities in the North Island, even as far away as Auckland or Wellington. Ashfall >1 cm in thickness may even occur in the upper South Island for these large eruptions at significant probabilities (>30%). Particular weather conditions result in increased probabilities of ashfall in different locations. Light winds associated with a high pressure system over New Zealand generally lead to the thickest accumulations of ash in the central North Island and the highest probability of ashfall at major cities. In contrast, strong dominant westerly winds lead to a significant amount of ash being distributed offshore into the Pacific Ocean.

Introduction

Caldera volcanoes are widely considered amongst the most destructive volcanoes on Earth and are typically associated with voluminous explosive eruptions that have multiple associated hazards including widespread ashfall and large pyroclastic density currents (*Blong*, 1984; *De Natale et al.,* 2017). At an extreme, the largest explosive events (termed supereruptions) eject >450 km^3 magma, with accompanying caldera collapse and global-scale impacts (*Self*, 2006). However, recurrence rates of such events are extremely low (1 every ~120-200 kyr: *Mason et al*., 2004). Most caldera volcanoes, including those that have hosted supereruptions, have widely diverse eruptive records with smaller but more frequent events typically ranging over several orders of magnitude from small dome building episodes (<0.01 km^3 magma) to moderate-volume (0.1-10 km^3) Plinian eruptions (e.g. among many examples: Long Valley: *Hildreth*, 2004; Campi Flegrei: *Di Vito et al*., 1999; Yellowstone: *Christiansen*, 2001; Aira: *Aramaki*, 1984); Taupo: *Wilson*, 1993; Santorini: *Druitt et al.,* 1999). The wide potential range of eruption sizes and the unpredictable nature of caldera volcanoes therefore make their hazard assessment inherently difficult (*Thompson et al.,* 2015). In addition, the reputation of calderas and the public perception of supervolcanoes mean that future unrest events, even the majority that do not result in an eruption, could generate significant social disruption (*Dominy-Howes and Minos-Minopoulos*, 2004; *Hill and Prejean*, 2005; *Lowenstern et al.*, 2006; *Potter et al.,* 2015).

Taupo is a large caldera volcano in the central North Island of New Zealand and the site of the most recent supereruption on Earth where >1,100 km^3 of pumice and ash was spread over the landscape at ~25.4 ka (*Wilson*, 2001*; Van Eaton et al*., 2012*; Vandergoes et al*., 2013) (Figure 1a). At least 25 smaller rhyolite eruptions have occurred at Taupo over the past 12,000 years and range in size over 3-4 orders of magnitude (Figure 1b). The largest and most recent eruption devastated a large portion of the North Island around 232 AD (*Wilson and Walker*, 1985*; Wilson*, 1993*; Hogg et al*., 2012). Minor changes in erupted magma chemistry over the past 12,000 years have been interpreted to reflect changing storage conditions in an evolving magma reservoir beneath Taupo (*Barker et al*., 2015). The distribution of inferred vent locations and range of model depths for magma storage also indicate that the modern magmatic system has rebuilt to a substantial size with >200 km^3 and plausibly up to 1000 km^3 of crystal mush that is capable of generating eruptible magma volumes on timescales of human interest and concern (*Barker et al*., 2015, 2016). Furthermore, minor unrest episodes have occurred roughly once per decade since 1870 (*Potter et al*., 2015) and geophysical evidence for unrest in 1982-83 has been linked to

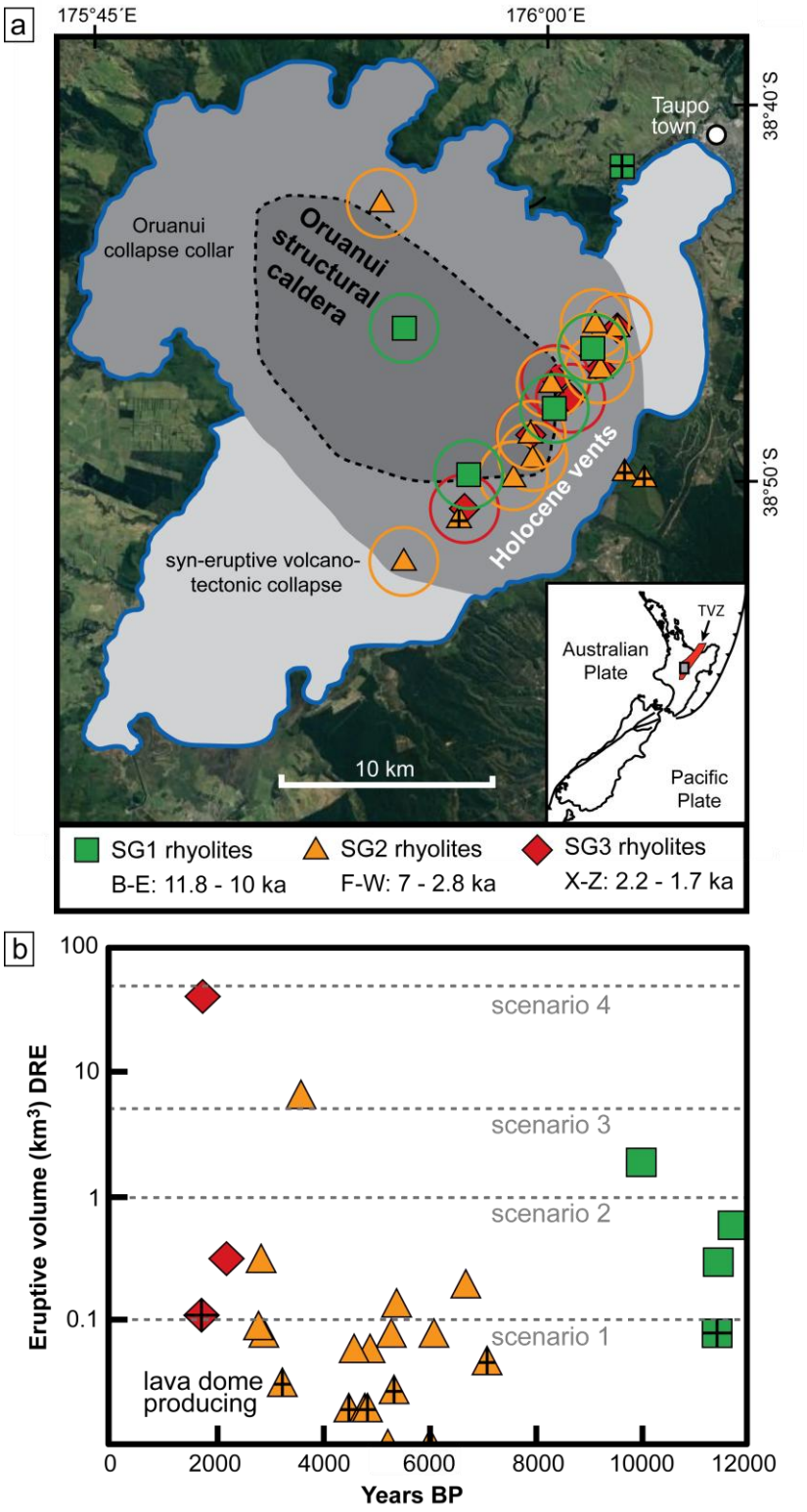

Figure 1. *(a) Map of the modern Lake Taupo and structural and volcanic features of Taupo caldera (map inset). Vent sites with approximate error ellipses and ages for post-Oruanui eruptions are after Wilson (1993). TVZ—Taupo Volcanic Zone; SG—subgroup. (b) Diagram showing erupted magma volumes in Dense Rock Equivalent (DRE) from Taupo over the Holocene. Grey dashed lines represent four of the five scenarios that have been adopted in this study for modelling purposes. Symbols marked with a cross represent eruptions that were dominantly effusive (see text for details).*

dewatering and movement of magma (*Smith et al*., 2007). Despite these recent findings there are no current estimates on how future potential eruptions from Taupo will impact New Zealand society or which regions are the most susceptible to damaging amounts of ashfall. Complexities arise from the wide range of past eruptive sizes, which have occurred after highly variable and un-related periods, as inferred from the geological record (*Wilson*, 1993; *Stirling and Wilson*, 2002) (Figure 2). With tectonic stress, mafic recharge and the state of the silicic mush influencing the timing and volume of eruptions from Taupo, it is inherently difficult to predict future activity and its potentially overwhelming impacts (*Rowland et al*., 2010; *Allan et al*., 2012; *Barker et al*., 2016).

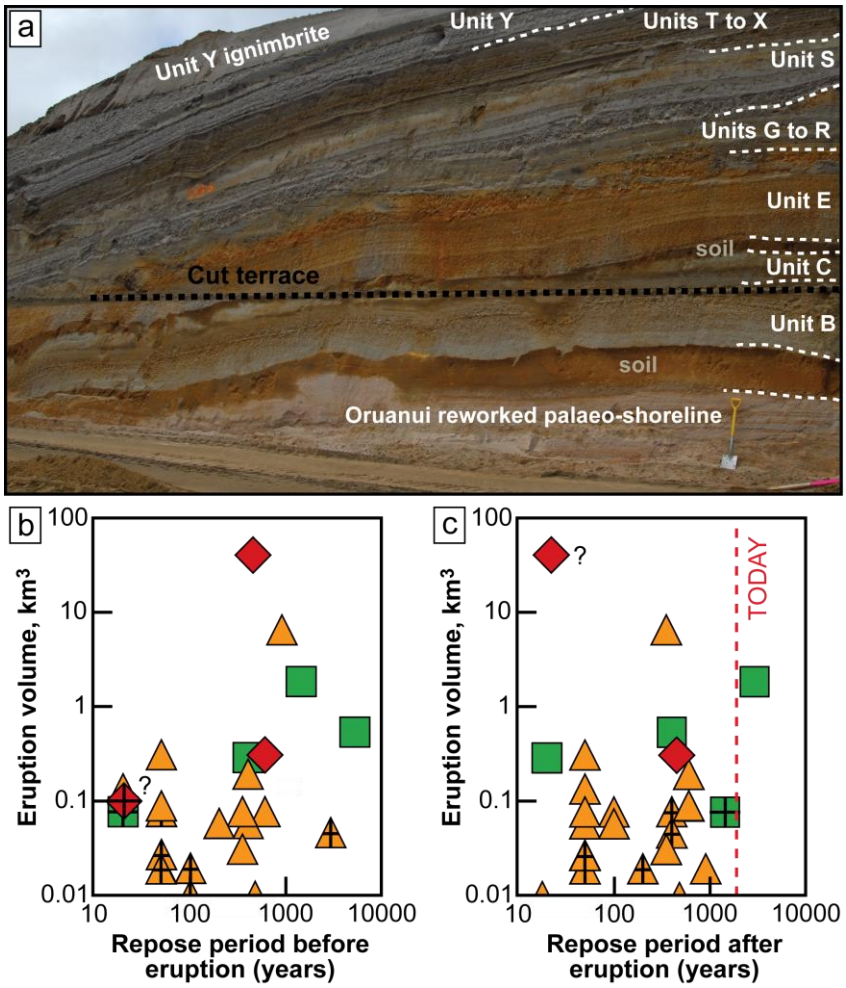

Figure 2. *(a) Photo of SH1 road cutting along the newly developed Taupo-bypass Highway 1 road showing the Holocene eruptive record from Taupo. White labels and dashed lines show the major eruptive units and bracketing palaeosols (soils) for reference. (b) Relationships between the volume of an eruption and the length of the repose period preceding an eruption or (c) following that eruption. Red dashed line shows today for reference. Age and volume data are from Wilson (1993). After Wilson et al. (2009). Symbols as in Figure 1.*

During recent eruptions in Europe (e.g., Eyjafjallajökull 2010 and Bardarbunga 2014-15), volcanic emissions have crippled air travel, infrastructures and the economy (*Langmann et al*., 2012). Even small eruptions as in 1995-96 at Ruapehu volcano, New Zealand, disrupted aviation and damaged communication networks, a hydro-electric power scheme, electricity transmission lines, water supply networks, wastewater treatment plants, agriculture and the tourism industry costing $NZ 130 million (in 1995/1996 value) (*Cronin et al*., 1998; *Johnston et al*., 2000; *Wilson et al*., 2012). Future eruptions from Taupo could be orders of magnitude larger than historic events at other New Zealand volcanoes, with voluminous ashfall potentially disabling the New Zealand economy. However, if a smaller event was to occur, impacts may be less widespread and disruptive. Given the geological record, what eruptive volumes and styles might we expect from future activity at Taupo and how would ash from a modern eruption disperse through the atmosphere? How variable could ash distribution be with New Zealand's dynamic weather patterns and what regions would be most susceptible to significant accumulations of ash?

In order to answer such questions, for this EQC biennial grant project we have combined our current understanding of Taupo's volcanic and magmatic history with numerical ash dispersal simulations to investigate how volcanic ash from a future event

would deposit across the modern New Zealand landscape. To address the complexities of variable eruptive sizes and conditions we use a scenario-based approach (e.g. *Costa et al.,* 2009; *Davies et al.,* 2015) and adopt a spectrum of volumes and eruptive parameters based on Taupo's geological record. By combining thousands of model simulation results with a modern understanding of weather patterns in New Zealand (*Kidson*, 2000) we calculate probabilities of ashfall across New Zealand and investigate the unique roles of eruption size and dynamic weather patterns on ash dispersal.

Research objectives and outcomes

Our proposed research had three main objectives (*in italics*) and resulted in the following outcomes (in plain text):

1. *Estimate the range of potential future eruption sizes from Taupo volcano, constrained by the latest chemical and physical studies of its magmatic system. We will build upon previous studies by identifying a statistically plausible range of eruption durations and volumes, from small (<1 km^3) through to large (>500 km^3), using field constraints from past eruptions to estimate the range of eruption intensities and durations. We will additionally identify seasonal intervals of 3-D, time-changing wind fields over New Zealand from modern meteorological data.*

We utilized a scenario-based approach based on the plausible range of eruption sizes that may be expected from a future event at Taupo caldera (Table 1). Our scenarios are motivated by two key considerations. The first consideration is based on the fact that Taupo eruptive volumes through the Holocene have varied from <0.01 km^3 to ~35 km^3 DRE (dense rock equivalent) (Figure 1b). The smallest eruptions were likely accompanied by effusive lava dome formation, often with preceding explosive eruptions (Figure 2b,c; *Wilson*, 1993). For modeling we consider explosive activity only, and place our smallest event (Scenario 1) at 0.1 km^3 DRE, of which there are ~11 Holocene examples (Table 1). To account for larger events we adopt size ranges from the geological record using 1 km^3, 5 km^3 and 50 km^3 (scenarios 2, 3 and 4 respectively; Figure 1b). The second consideration is based on magmatic records from geochemical studies that indicate a substantial volume of partially molten crystal mush may be present beneath Taupo (*Barker et al*., 2015). Although considered to be a first-order estimate and in need of confirmation by geophysical observations, up to 1000 km^3 of crystal mush could hypothetically generate an eruptible melt body larger than any Holocene event and potentially of similar volume to the Oruanui supereruption as an end-member event. We therefore define the maximum credible event as a 500 km^3 supereruption, as defined by Scenario 5 (Table 1), but emphasize the extremely low probability of such an event occurring (*Stirling and Wilson*, 2002).

Table 1. *Summary of eruption scenarios and inputs used in Ash3d simulations*

Parameter(s)	Scenario 1	Scenario 2	Scenario 3	Scenario 4	Scenario 5
Erupted volume, km^3 DRE	0.1	1	5	50	500
Number of Holocene eruptions of similar size	11	6	2	1	0
Annual probability from Stirling & Wilson 2002	0.1%	0.03%	0.01%	<0.01%	<<0.01%
Umbrella cloud?	no	yes	yes	yes	yes
Plume or Umbrella Cloud top height, km	15	15	20	20	20
Duration, hrs	6	12	24	24	72
MER (kg/s)	1.16E+07	5.79E+07	1.45E+08	1.45E+09	4.82E+09
Nodal spacing	0.25° horizontal 2.0 km vertical	0.25° 2.0 km	0.35° 2.0 km	0.35° 2.0 km	0.35° 2.0 km
Diffusion coefficient D_x	0	0	0	0	0
Suzuki constant *k*	8	12	12	12	12
Analagous eruption examples with measured parameters	Soufriere St Vincent 1902, MSH 1980 May ***upper VEI4***	Redoubt 2009 (event 5), Hudson 1991 (Chile) ***VEI5***	Pinatubo 1991, Quizapu 1932, Santa Maria 1902, Novarupta 1912 ***VEI6***	Taupo 232AD, Tambora. Caldera collapse ***VEI7***	Oruanui 25.4 ka, Bishop Tuff Supereruption ***VEI8***

Within each of the five eruptive scenarios we have selected eruption durations as constrained by both the geological record at Taupo and similar sized historic eruptions worldwide where the MER (mass eruption rate) has been estimated (Table 1). MER is an extremely important input and may be highly variable for eruptions of the same volume as demonstrated by historic events, but generally scales with total eruption volume so that larger eruptions have higher MER and their plumes reach higher levels (*Carey and Sigurdsson*, 1989; *Mastin et al*., 2009, their Figure 1). At Taupo, with the exception of a few examples, such as the early part of the 232 AD eruption, most of the eruptions in the geological record appear to be continuous and occurred over periods of hours to tens of hours (*Wilson*, 1993; *Rhoades et al.,* 2002). For the smallest eruption scenario (0.1 km^3) we have selected duration of 6 hours, resulting in an MER of ~1 x 10^7 kg/s and a plume that reaches 10 km height (*Mastin et al*., 2009). For larger eruptions we have increased the umbrella height and MER to match examples with similar erupted volume (Table 1). Umbrella heights are within the lower limits of those calculated from Taupo isopleth data (*Carey and Sparks*, 1986; *Wilson*, 1993), increasing from 15 km for Scenario 2 to 20 km for the larger eruptions.

Eruption durations are not well constrained for the scenarios 4 and 5 due to the rarity of such eruptions and the wide range of possible conditions. For the purpose of model simplicity we have used high MER with a total duration of 24 hours for scenario 4 and 72

hours for scenario 5. For scenario 4, similar plume heights and MER were calculated for the 1815 Tambora eruption, where although the total eruption occurred over more than a week, the majority of the 50km^3 DRE volume was erupted over 24 hours (*Self et al*., 1984; *Sigurdsson and Carey*, 1989; *Oppenheimer,* 2003). For scenario 5 we have used the 760 ka Bishop Tuff supereruption as an extreme example, which is inferred to have mostly erupted over ~90 hours (*Wilson and Hildreth*, 1997). We note that in both the cited analogous examples a large proportion of the ejected material formed pyroclastic flows or co-ignimbrite fall and therefore consider these scenarios as being open to a large window of variability and our selected conditions likely represent maximum MER and ash distribution for the given volume.

For particle inputs we use a grainsize distribution modified from the 1980 Mount St. Helens eruption (*Durant et al*., 2009), but modified by *Mastin et al*. (2016) to account for ash aggregation by consolidating the fine ash into aggregate size classes that were fine-tuned to match four diverse eruption deposits . We adopt this size distribution due to similarities to those estimated from the 232 AD Taupo eruption (*Walker,* 1980). The size distribution and density of aggregates were derived by systematic adjustment to optimize fit with mapped deposits (*Mastin et al.*, 2016). One affect of using this size distribution which does not include particles coarser than 2 mm is that model thicknesses will underestimate the most proximal values (*Mastin et al.,* 2016). To calculate particle densities we assume 65% vesicularity for 2 mm ash based the upper tail of pumice density histograms from Taupo (*Houghton et al*., 2010) that corresponds to a bulk density of ~800 kg/m^3. We then increase the particle density by 200 kg/m^3 every 0.5 *phi* size step down to 88 microns, where the total material in this size bin has a mean density of ~2600 kg/m^3, assuming that the glass in 80% of the deposit at ~2400 kg/m^3 and crystals and lithics make up the remaining 20% at ~2900 kg/m^3. Ash3d calculates settling velocities using the formula of *Wilson and Huang* (1979), which considers ellipsoidal particles with a shape factor $\boldsymbol{F} \equiv (\boldsymbol{b}+\boldsymbol{c})/2\boldsymbol{a}$, where $\boldsymbol{a}$, $\boldsymbol{b}$, and $\boldsymbol{c}$, are the semi-major, intermediate, and semi-minor radii of a 3-D ellipsoid. For particles, we use $\boldsymbol{F}$ = 0.44, which is the average measured by *Wilson and Huang* (1979) for natural pyroclasts. For aggregates we assume F = 1 (round aggregates).

An important aspect of this study is to consider how different weather patterns would affect ash dispersal. Unlike larger continents, New Zealand's maritime climate in the South Pacific Ocean leads to highly variable wind patterns that do not show a pronounced seasonality. Instead, the synoptic conditions are classified by "Kidson types" to describe the 12 most common weather patterns (*Kidson*, 2000) (Figure 3). Here we use the Kidson

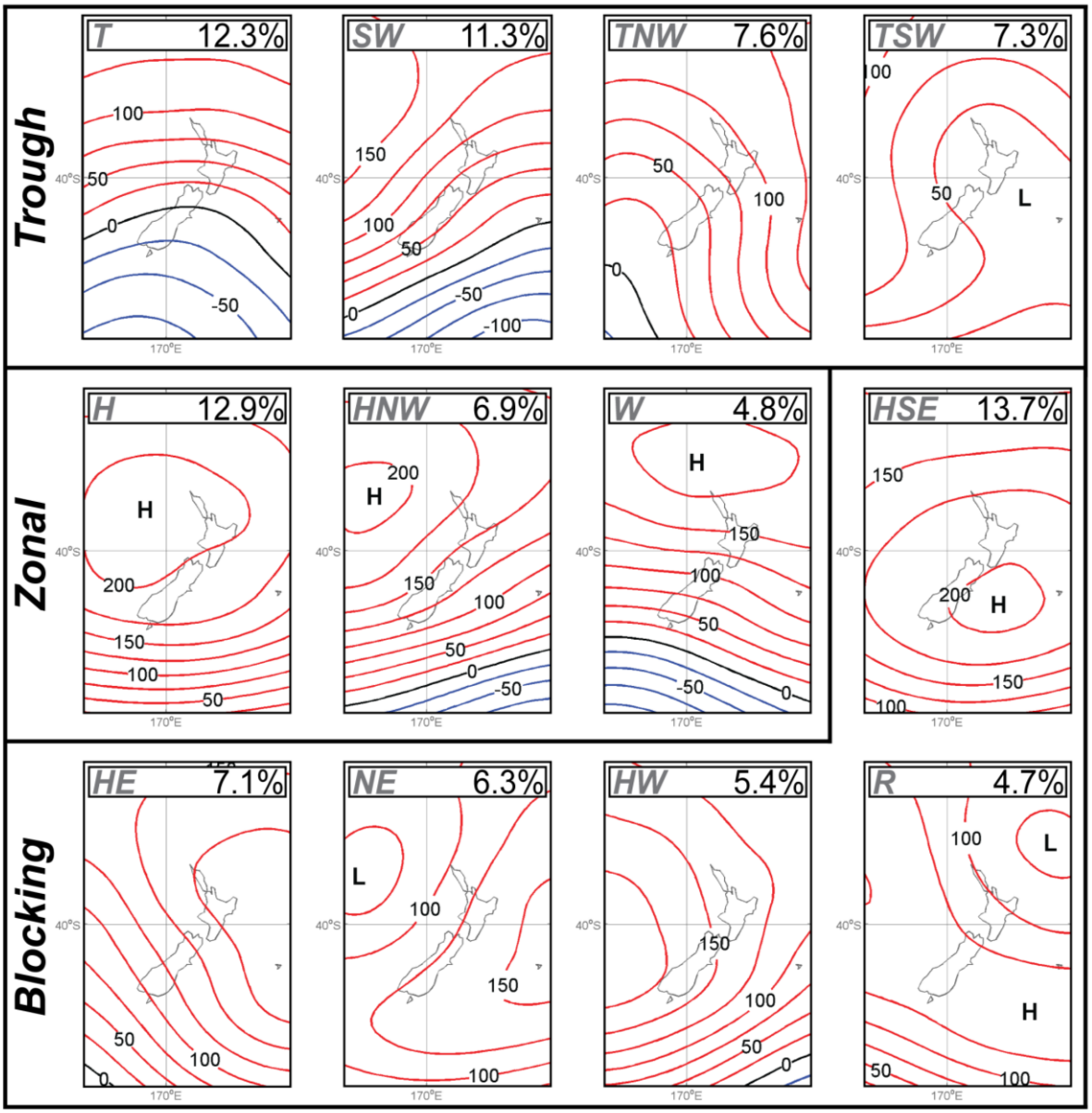

Figure 3. *The twelve Kidson weather classifications, shown as average patterns of the height of the 1000 hPa (mean sea-level pressure) isobar. Names for the synoptic types are indicated in the top left of each panel (see text for details). The three main regimes are indicated at the left. See Kidson (2000) for further details.*

classification to further investigate the impact of variable weather regimes on ash dispersal for the five different sized eruptive scenarios. Kidson classifications are based on cluster analysis of 12-hourly (00 and 12UTC) 1000 hPa height fields using data from NCEP/NCAR reanalysis 1 (RE1) back to 1949 (*Kalnay et al.,* 1996). Each Kidson type typically occurs for 1-1.5 days on average and only some types show seasonal variability (*Kidson*, 2000; *Renwick*, 2011). Kidson types are divided into three main weather regimes as determined by the position of low and high pressure systems around New Zealand (Figure 3):

1) Trough regime, whereby an unsettled trough system is over New Zealand or towards the east and results in mostly NW or SW wind flow, reduced temperatures and increased precipitation (*Renwick*, 2011).

2) Zonal regime, in which a high pressure system is centered above or to the NW of New Zealand resulting in east to west wind flow but drier conditions in the North Island.

3) Blocking regime, where a high pressure system sits to the south of New Zealand, resulting in less wind but variable direction, depending on the position of the high, wetter conditions in the NE of New Zealand and drier conditions in the SE.

RE1 data used in the cluster analysis of *Kidson* (2000) are provided at 2.5° intervals on a lat/long grid, with 17 vertical pressure levels up to ~34 km above sea level and have also been used here as the meteorological input for Ash3D modeling. Higher resolution data from the European Reanalysis (ERA) (1° intervals) and WRF (0.1° intervals) are available but require substantially longer computing times and were found to have little effect on overall ash distribution when directly compared with models using RE1 data. The RE1 database also has the benefit of having the greatest historical coverage back to 1949, allowing broader representation of the weather patterns and El Niño Southern Oscillation (ENSO) cycles that can significantly affect New Zealand's wind fields and the dominant Kidson types (*Jiang et al.,* 2004; *Renwick,* 2011).

2. *Investigate the nature and extent of ash dispersal resulting from a feasible range of eruption scenarios, using the most advanced dispersal model available, Ash3d, hosted by the United States Geological Survey. Ash3d has been previously tested on multiple volcanic eruptions, including a future supereruption from Yellowstone caldera. Our study will build upon previous studies using Ash3d to establish the ashfall dispersal and fallout from a future eruption of Taupo volcano in a way that is explicitly constrained by geological data. By integrating seasonal variations in wind speed in New Zealand's unique atmospheric conditions, our study will provide the most advanced ashfall prediction models ever applied to New Zealand volcanoes*.

We have modeled atmospheric transport and deposition of ash using the dispersal model Ash3D, a finite-volume Eulerian model that is particularly well adapted for large explosive eruptions (e.g. *Schwaiger et al.*, 2012; *Mastin et al.* 2014). Rather than resolving the near-source dynamics of the volcanic plume, Ash3d specializes in long-range transport in a 3-D, time-changing wind field. To capture the effects of New Zealand's dynamic atmosphere, the model uses historic meteorological data (RE1) covering the full range of regional weather patterns (*Kidson*, 2000: Figure 3). Ash3D calculates tephra transport through the atmosphere by dividing it up into a three-dimensional grid of cells and calculates the mass flux through cell walls as tephra is advected by wind and falls at a settling velocity determined by the shape, size and density of the particles (*Schwaiger et al.*, 2012; *Mastin et*

al. 2014). For eruptions >0.1 km^3 in volume we have used a modified version of Ash3D that accounts for the growth of an umbrella cloud (*Mastin et al*., 2014), a feature that is expected from eruptions of this size at higher MER. For each eruption scenario outlined in Table 1 and described above, we completed 1,000 model simulations that randomly sampled different dates and times in the RE1 weather database between 1949 and 2016. Each individual run was then assigned with a percentage of each Kidson weather regime (Figure 3), based on 6 hourly sampling across the eruption duration and allowing for total fallout from the plume for an additional 8 hours after the end of eruption when >99% of ash was deposited. The majority of model simulations span multiple Kidson weather regimes, especially for the larger eruption scenarios that span 24-72hrs.

Results from individual model simulations vary significantly, both within and between eruptive scenarios, highlighting the effects of both increasing eruption intensity and day-to-day weather patterns on overall ash dispersal (Figures 4 and 5). For simulations of the smallest eruption volume of 0.1 km^3 (Scenario 1: Figure 4a), the lower MER and lack of umbrella cloud results in very little ash being deposited up-wind. Strong winds result in significantly narrow ash dispersal and carry the majority of the ash offshore (Figure 4d,h), mostly to the east of New Zealand with the dominance of westerly winds in the central North Island. With increasing MER for 1 km^3 (Scenario 2) and 5 km^3 (Scenario 3) eruptions under the same weather conditions, the growth of an umbrella cloud results in more ash being carried up-wind in light winds, such as those experienced during zonal or blocking weather regimes (e.g. Figure 4b,c). Strong westerly winds still carry the majority of the ash offshore in these larger eruptions (Figure 4e,f) but there is greater cross-wind deposition with increasing eruption size and higher MER. For example, the cross-wind deposition of ash on the eastern edge of the North Island between Napier and Gisborne increases substantially with the larger eruption sizes from 130 km to 230 km to 330 km for eruptions of 0.1 km^3, 1 km^3 and 5 km^3, respectively (Figure 4d-f). For the largest eruptions considered here in Scenario 4 (50 km^3) and Scenario 5 (500 km^3), significantly more ash is deposited both up-wind and cross wind in all examples shown (Figure 5). However, strong winds still significantly skew ash thickness contours, even at the highest MER associated with such events (Figure 5c-d). In many cases, transitional weather patterns result in deposit maps that show bilobate or complex final distributions (Figure 4h-j, Figure 5e-f). On an individual basis, each model simulation and the resulting eruptive deposit maps are highly sensitive to the start time of the eruption and the wide range of possible wind conditions and associated weather regimes.

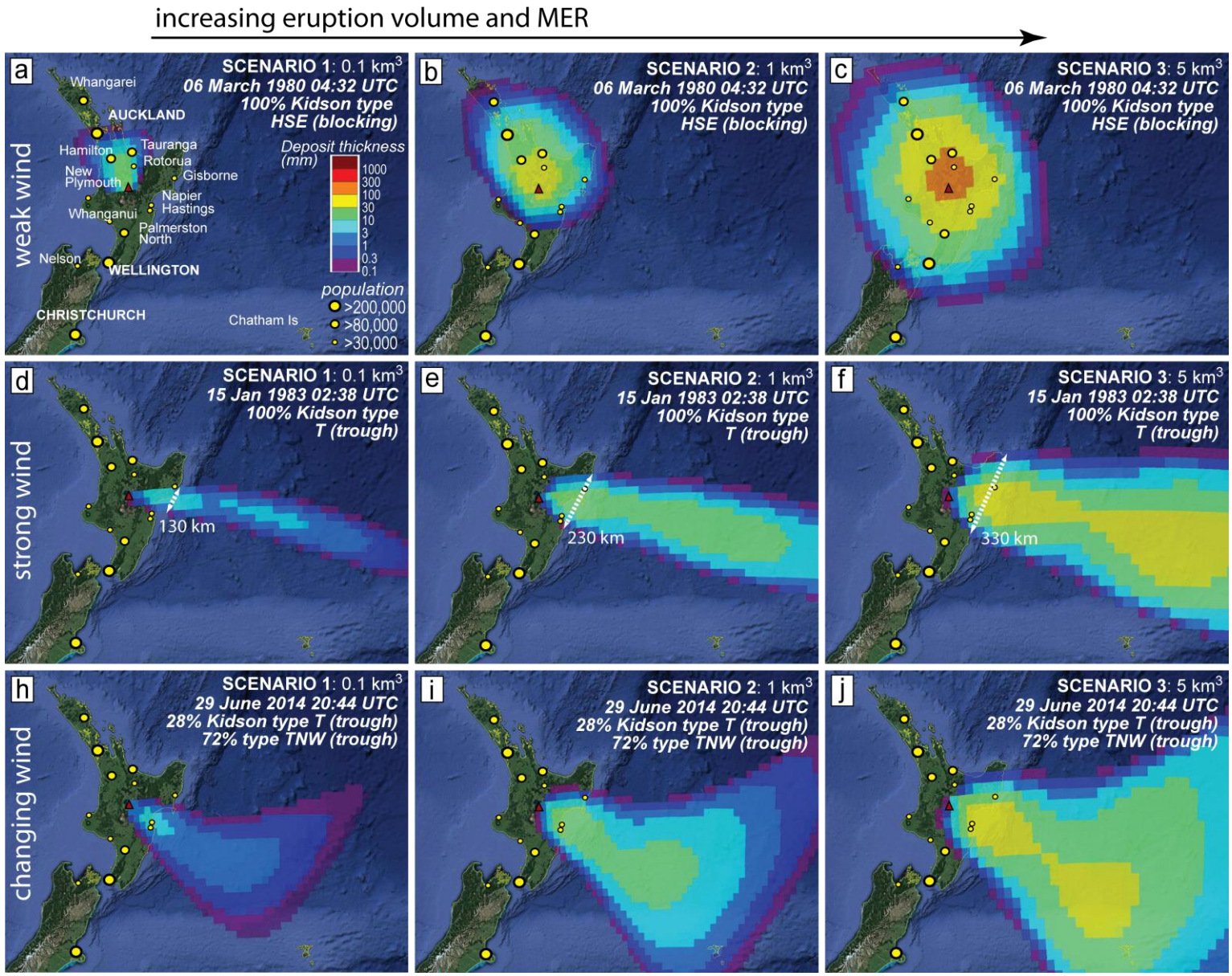

Figure 4. *Selected examples of model outputs from individual Ash3d simulations showing final ash deposit thickness (0.1 mm minimum) across New Zealand. Diagrams from left to right show increasing eruption sizes from scenarios 1-3 (0.1 km^3 to 5 km^3 erupted volume) but with the same eruption start times and weather conditions such that (a) to (c) show constant light wind conditions, (d) to (f) show constant strong westerly wind conditions and (h) to (j) show changing wind conditions. The percentage of synoptic Kidson weather regime from Figure 3 and start date and time of the eruption are shown at the top right of each panel. Major population centres are labelled in (a) for reference. See text for further details and Table 1 for details on the eruption scenarios. Base maps are from © 2018 Google Earth.*

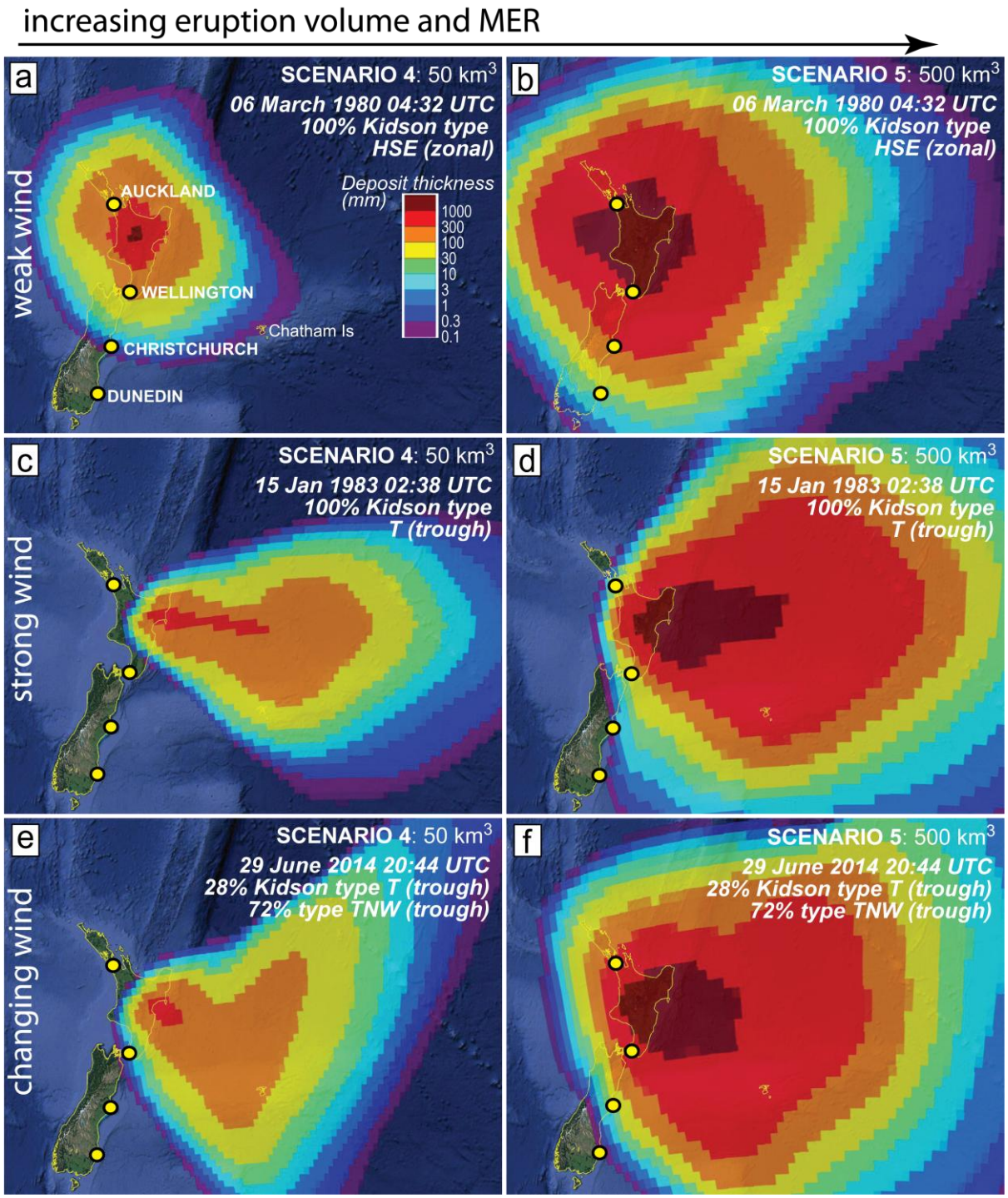

Figure 5. *Selected examples of model outputs from individual Ash3d simulations showing final ash deposit thicknesses across New Zealand. Diagrams from left to right show increasing eruption sizes from scenarios 4-5 (50 km^3 to 500 km^3 erupted volume) but with the same eruption start times and weather conditions such that (a) and (b) show constant light wind conditions, (c) and (d) show constant strong westerly wind conditions and (e) to (f) show changing wind conditions. All other details as in Figure 4.*

3. *Generate a series of useful ashfall hazard probability maps for the various eruption scenarios to calculate a 'worst case scenario' and to identify specific geographical areas most likely to be affected by ashfall. For ongoing hazard management studies stemming from this proposal, the hazard maps will form the basis to estimate risk to critical infrastructure to quantify the likely impacts of Taupo ashfall on New Zealand's society and economy. These scenarios will also form an important part of future emergency management and risk-management planning exercises and programmes.*

To generate probabilistic maps, all 1000 model simulations were combined to produce thickness-probability contours at 60%, 30%, 10% probability levels and the 1% limit for each eruptive scenario (Figures 6, 7, 9). For the 0.1 km^3 eruption size (Scenario 1), deposits exceeding 1 cm thickness are mostly confined to proximal locations (<100 km from vent) in the central North Island at the 10% probability level and only major towns located 200-300 km from vent fall within the 1% limit (Figure 6a). Probability contours of >1 mm ashfall for Scenario 1 are strongly skewed to the east, highlighting the dominance of westerly winds in the central North Island, with major population centres to the northeast and southeast of Taupo falling into the 10-30% range of probabilities (Figure 6b).

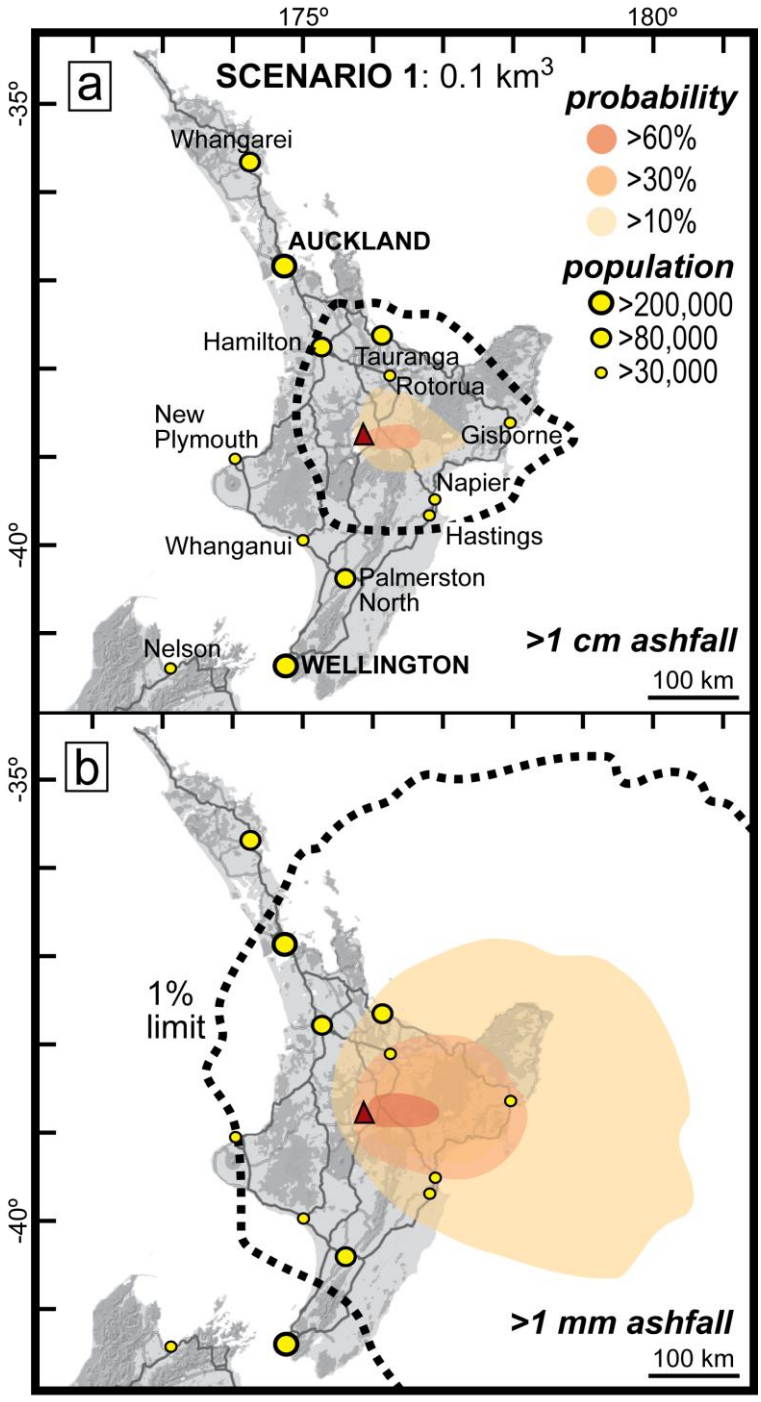

Figure 6. *Probability maps produced from 1000 Ash3d model simulations showing probability contours of ash deposits across the North Island for eruption Scenario 1 (0.1 km^3) exceeding (a) 1 cm thickness and (b) 1 mm thickness. Locations of major population centres are labelled in (a) for reference. The black dashed line represents 1% limit where 99% of the simulations contained ash at the specified thickness within this boundary (see text for discussion). Background map in greyscale is from © 2018 Google Maps, with dark grey lines representing major highways.*

For the 1 km^3 eruption size (Scenario 2), probability contours become less ellipsoidal as a result of increasing cross-wind and up-wind deposition with the growth of an umbrella cloud at higher MER (Figure 7). At >1 cm thickness, the 60% probability contour for Scenario 2 covers a much wider area across the eastern central North Island out towards the cities of Napier and Gisborne on the east coast (Figure 7a). Auckland city falls within the 10% probability contour for >1 mm ashfall and all major population centres across the North Island fall within the 1% limit for Scenario 2 (Figure 7b). For the 5 km^3 eruption size (Scenario 3), all centres in the eastern North Island fall within the 60% probability contour and all other population centres in the North Island have significant probabilities (>10%) of ashfall >1 mm (Figure 7c).

For the largest eruptions considered here, probability contours are more circular and cover parts of the South Island for deposits of 10 cm and 1 cm thickness (Figure 8). In the 50 km^3 eruptions, (Scenario 4) the whole central and eastern North Island is covered by

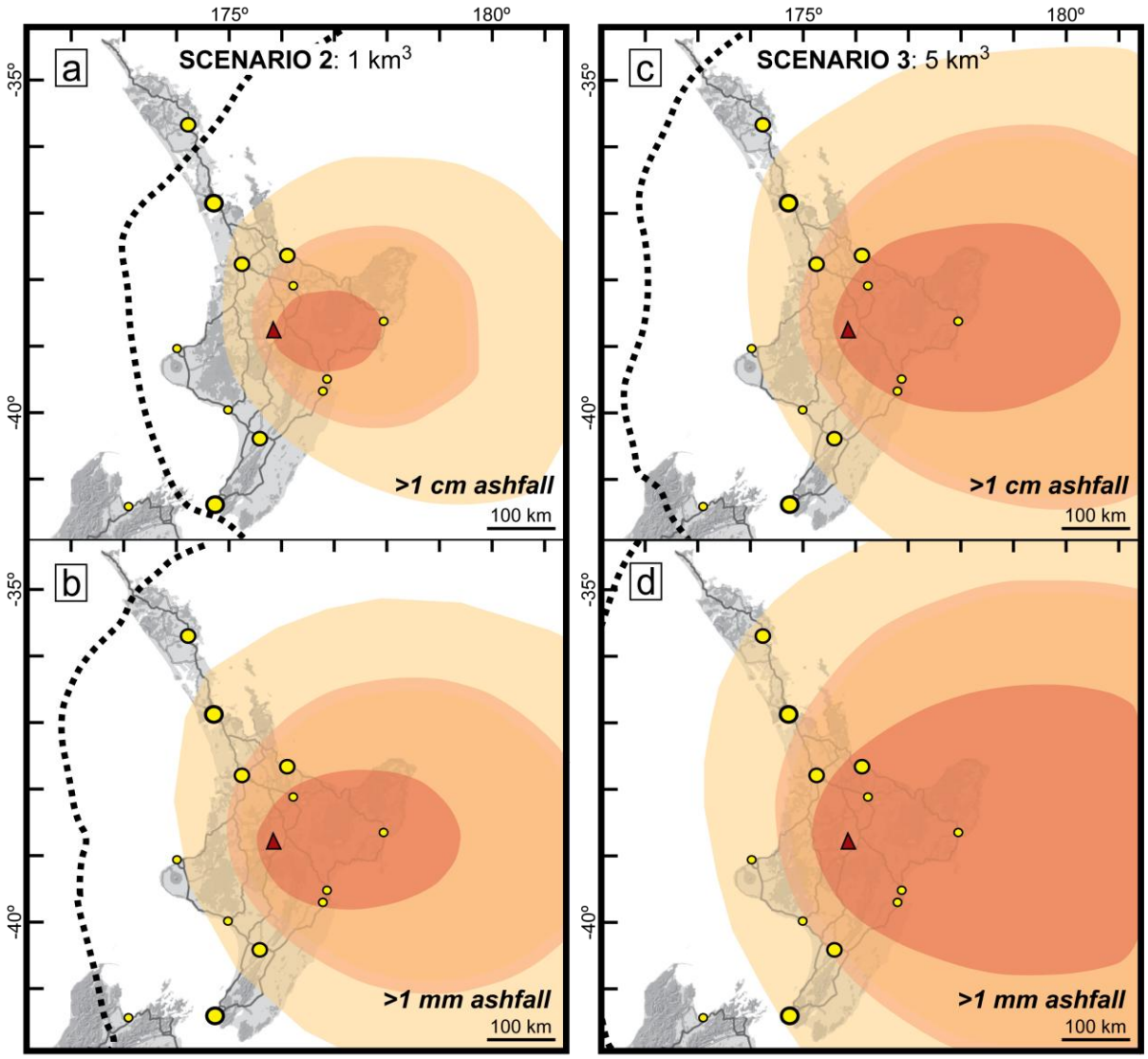

Figure 7. *Probability maps produced from 1000 Ash3d model simulations showing probability contours of ash deposits across the North Island exceeding (a) 1 cm thickness and (b) 1 mm thickness for eruption Scenario 2 (1 km^3) and exceeding (c) 1 cm thickness and (d) 1 mm thickness for eruption Scenario 3 (5 km^3). All other details as in Figure 6.*

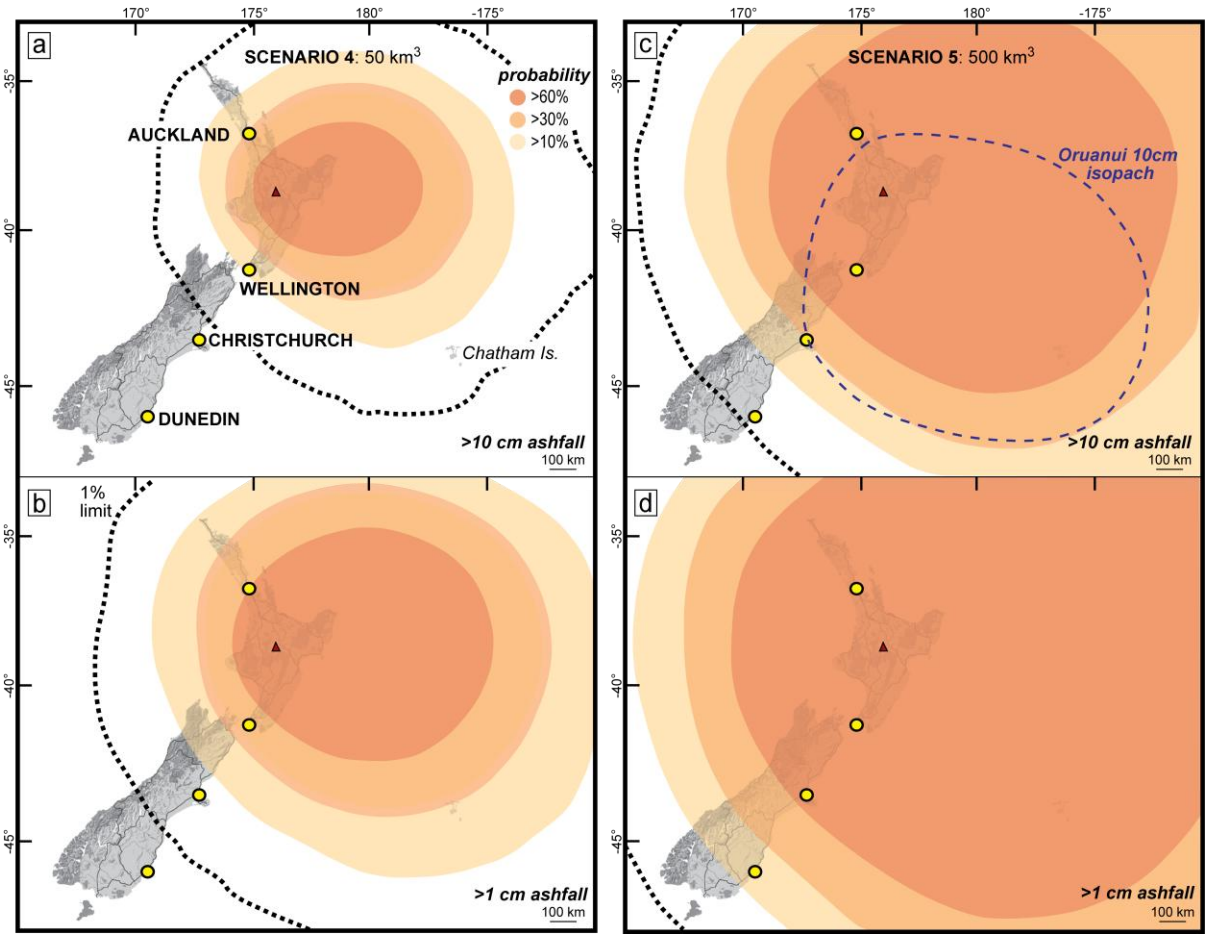

Figure 8. *Probability maps produced from 1000 Ash3d model simulations showing probability contours of ash deposits across New Zealand exceeding (a) 10 cm thickness and (b) 1 cm thickness for eruption Scenario 4 (50 km^3) and exceeding (c) 10 cm thickness and (d) 1 cm thickness for eruption Scenario 5 (500 km^3). All other details as in Figure 6. Note the change in scale and order of magnitude increase in deposit thicknesses when compared to Figure 6 and 7.*

the 60% probability contour at 10 cm thickness, with Auckland and Wellington at ~30% and 10% probability, respectively (Figure 8a). For the 500 km^3 supereruption (Scenario 5) the entire North Island and Pacific ocean out to the Chatham Islands is enclosed within the 60% contour at 10 cm thickness and in the South Island Christchurch city falls on the 30% probability contour (Figure 8c). The published 10 cm isopach from the Oruanui supereruption covers a broadly similar total area and shape to the 60% probability level, though it is more skewed to the southeast (*Wilson*, 2001).

Probability-thickness plots for major population centres located in different geographical locations around the North Island highlight which areas have the highest probability of ash accumulation at any given thickness down to trace levels (0.1 mm) for each eruptive scenario (Figure 9). For reference only, we have also plotted three different damage threshold thicknesses from *Jenkins et al*. (2015) to show what ash thickness can be expected to cause minor damage but significant crop losses and clean-up costs (20 mm), total crop losses and major repairs to infrastructure (100 mm) and structural collapse of most timber-framed roofs (300 mm). Due to the dominant westerly winds (Figure 3), the

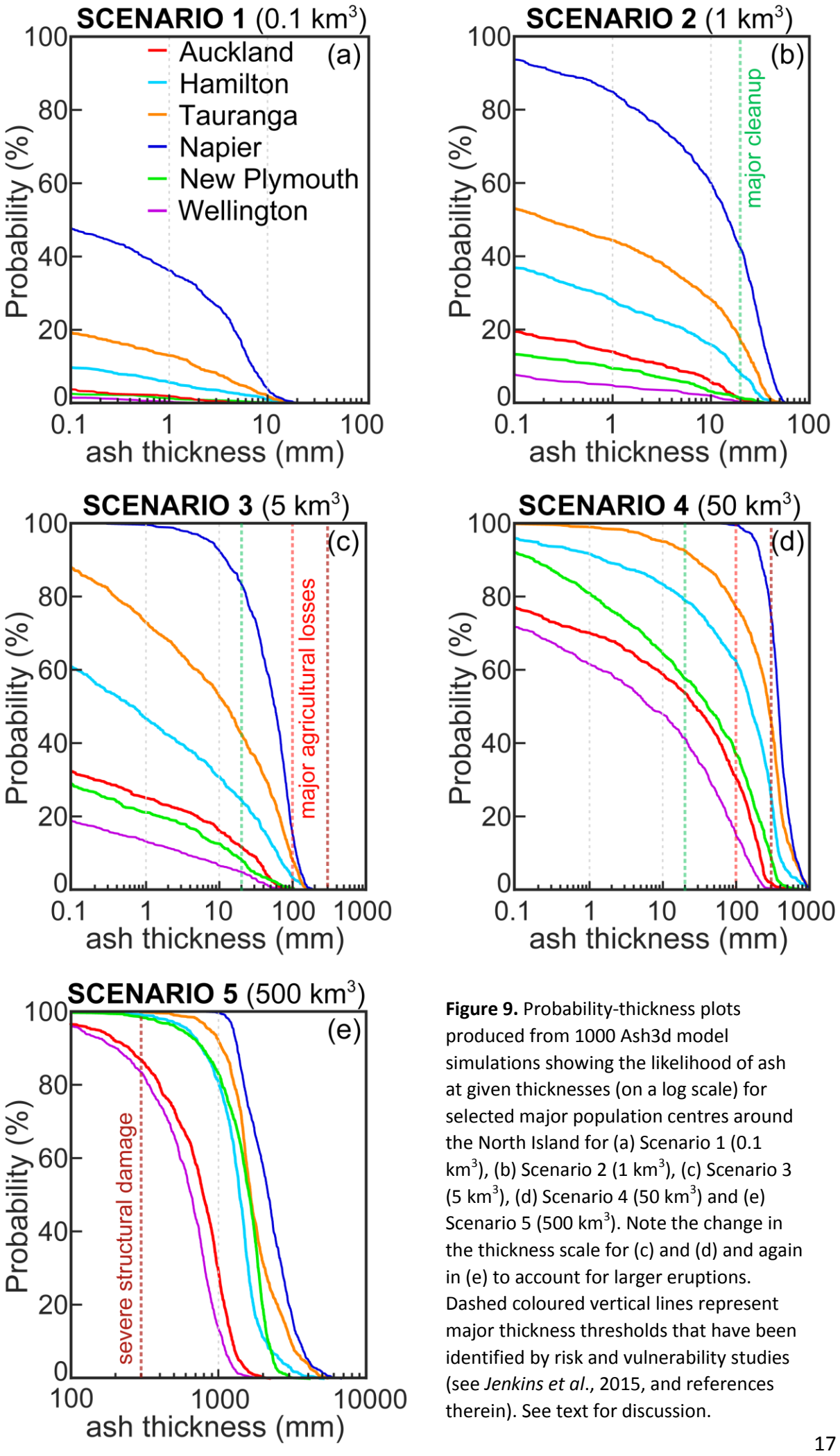

Figure 9. Probability-thickness plots produced from 1000 Ash3d model simulations showing the likelihood of ash at given thicknesses (on a log scale) for selected major population centres around the North Island for (a) Scenario 1 (0.1 km^3), (b) Scenario 2 (1 km^3), (c) Scenario 3 (5 km^3), (d) Scenario 4 (50 km^3) and (e) Scenario 5 (500 km^3). Note the change in the thickness scale for (c) and (d) and again in (e) to account for larger eruptions. Dashed coloured vertical lines represent major thickness thresholds that have been identified by risk and vulnerability studies (see *Jenkins et al.*, 2015, and references therein). See text for discussion.

Table 2. *Average arrival times of ashfall at selected major population centres around the North Island of New Zealand for the five different sized eruptions scenarios considered*

Scenario	**1**		**2**		**3**		**4**		**5**	
Size	0.1km^3 (no umbrella)		1km^3		5km^3		50km^3		500km^3	
City	mean (hrs)	σ	mean	σ	mean	σ	mean	σ	mean	σ
Auckland	8.4	2.6	9.1	3.8	13.9	7.8	11.1	7.4	8.5	9.0
Hamilton	6.1	2.4	7.1	4.0	10.2	7.4	5.4	5.4	2.1	2.0
Tauranga	5.2	2.9	5.4	3.7	6.1	5.9	2.3	2.8	1.2	0.5
New Plymouth	7.7	2.9	9.5	4.0	15.8	7.8	10.4	7.0	3.9	3.1
Napier	3.5	2.5	3.5	3.0	3.0	3.0	1.2	0.5	0.9	0.1
Wellington	10.7	2.5	11.1	4.1	15.7	7.1	13.9	7.4	11.5	10.4

city of Napier on the east coast of the North Island has the highest probability of >0.1 mm ashfall with ~50% probability for Scenario 1 (Figure 9a), ~95% for Scenario 2 (Figure 9b) and >99% for all larger eruptions (Figure 9c-e). Typical thicknesses that occur in Napier increase drastically between eruption scenarios with 0.1-10 mm for Scenario 1, up to 50 mm for Scenario 2, ~10-100 mm for Scenario 3, 100-1000 mm for Scenario 4 and 1000-5000 mm for Scenario 5. To the north of Taupo, Tauranga has a probability of ashfall >0.1 mm of ~20% for Scenario 1, ~55% for Scenario 2, ~85% for Scenario 3 and >99% for scenarios 4 and 5. Notably, there is a significant shift in the shape of the probability-thickness curve for Tauranga between Scenario 3 and 4, with a high probability of ash thickness >100 mm in Scenario 4 (~80%) versus Scenario 3 (<10%) (Figure 9c-d). Similar shifts in the probability curve occur for the city of Hamilton, which has >80% probability of ashfall >10 mm for Scenario 4, compared to <30% for Scenario 3. On the west of the North Island, New Plymouth has lower probabilities of ashfall than Auckland city for Scenarios 1-3 (Figure 9a-c), but then has slightly higher probabilities of ashfall than Auckland at any given thickness for Scenario 4 (Figure 9d) and much higher probabilities for Scenario 5 at all thicknesses (Figure 9e). Auckland and Wellington have the lowest probability of ashfall for the major centres, being located ~250 km northwest and ~300 km southwest from Taupo volcano, respectively. Significant ashfall (>10 mm) is indicated for these locations at lower probabilities (<20-30%) for Scenarios 1-3, but these double for Scenario 4 to 50-60% and large amounts of ashfall (>100 mm) occur at very high probabilities (>95%) for Scenario 5.

Calculated average arrival times shown in Table 2 indicate how long it takes for ash to start accumulating on the ground after the start of eruption for selected major centres around the North Island. Average travel times vary significantly from 1 to ~16 hours

depending on city location and eruption size. A major feature of Table 2 is that all major centres, apart from Napier, show an increase in average travel times from the smallest eruptions of 0.1 km^3 (Scenario 1) to the 5 km^3 eruptions (Scenario 3). In some cities like Auckland, Hamilton and New Plymouth, there is 150-200% change in travel times from Scenario 1 to 3. However, the standard deviation on the average times also increases significantly with larger eruption sizes, indicating a much wider spread in the individual simulation arrival times. Between the 5 km^3 eruptions (Scenario 3) and the larger 50 km^3 (Scenario 4) and 500 km^3 eruptions (Scenario 5), average travel times at all centres, including Napier, decrease back to similar or lower values than that calculated for the smaller eruptions, but with high standard deviations for distal locations, reflecting the wide diversity of wind directions covered within the 1000 simulations.

To investigate the effect of different weather patterns on ash dispersal, we assigned each individual Ash3d dispersal simulation with a percentage of the different particular synoptic Kidson regimes that it experienced, using the database of *Kidson* (2000). This assignment was based on 6 hour sampling intervals for the duration of the eruption and an additional 8 hours to allow for >99% ash deposition (Figure 4 and 5). The total sampling time for each simulation varies between the eruption scenarios due to the changing duration of the eruptions from 14 hours (6 hours eruption + 8 hours fallout) for Scenario 1 (0.1 km^3) to 80 hours (72 hours eruption + 8 hours fallout) for Scenario 5 (500 km^3) (Table 1). As each Kidson type lasts on average for 1-2 days (*Kidson*, 2000), the majority of the simulations contain a mixed percentage of synoptic classifications, especially for the larger eruptions with longer durations. Changing weather and thus mixed Kidson types can generate a wide variety of complex ash deposit thickness maps with multiple dispersal axes reflecting changing wind directions and strength (Figures 4h-j and 5e,f). To highlight the role of different weather regimes on ash dispersal, we isolated deposition maps that reflect relatively constant weather conditions that only experienced a single Kidson type (e.g. Figures 4 a-f and Figure 5a-d). This approach allows us to make broad inferences about how ash dispersal changes with the different weather regimes described by *Kidson* (2000) and pinpoint where ashfall would be most likely to occur in different wind conditions on any given day. As an example, Figure 10a shows the exceedance probability of ashfall occurring in Auckland at different thicknesses from a Scenario 3 (5 km^3) event using only those simulations that had 100% of any of the 12 different Kidson types. For Auckland, there is a much higher likelihood of thick ashfall occurring during Kidson types H and HSE when there are light winds resulting from a high pressure system situated close to or over mainland New Zealand. In contrast, there is a much lower probability of ashfall in Auckland during any

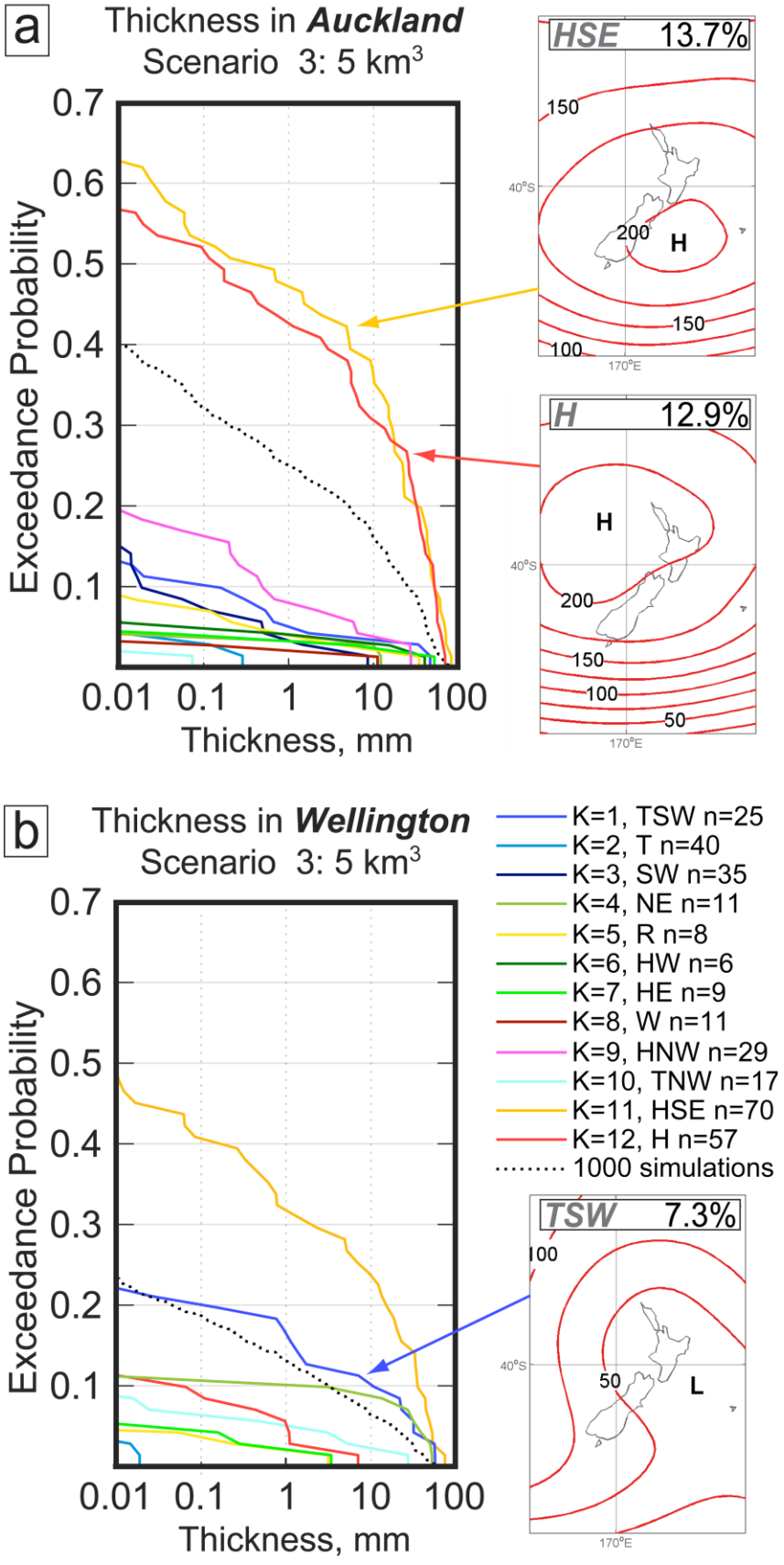

Figure 10. Exceedance probability-thickness plots produced from selected ashfall simulations for Scenario 3 (5 km^3) eruptions that experienced only a single particular Kidson weather classification type for (a) Auckland and (b) Wellington. The dotted black line represents all 1000 simulations for reference and includes simulations with mixed multiple Kidson types that represent complex and changing winds. Lines for selected Kidson types missing in (b) means there were no simulations of that particular Kidson type that produced ashfall in Wellington. Inset maps showing composite patterns of 1000 hPa height of Kidson synoptic types that generate the highest probability of ashfall are shown for reference from Figure 3 (*Kidson*, 2000). See text for discussion.

of the other Kidson types (Figure 10a). For Wellington, Kidson type HSE also results in a higher probability of ashfall along with Kidson types TSW and NE, which generate winds that put ash to the lower North Island. As the majority of the other Kidson types generate winds that blow from the W or SW, there is a much lower probability of ashfall occurring in Wellington during these weather classifications.

A summary of the different synoptic Kidson weather regimes and their generalized control on ash distribution from Taupo eruptions are given below (see Figure 3 for isobaric maps of Kidson classification types). These generalizations are for eruption scenarios 1 through 3 (0.1 km^3 to 5 km^3), while for larger eruptions the umbrella cloud may act to push a significant amount of ash upwind or crosswind (Figure 5).

Type 1 (TSW: 7.3%, no seasonal control): Dominantly light to moderate SW to NW winds that distribute ash over the eastern or southeastern lower North Island from the Hawkes Bay area and down to Wellington in some cases (e.g. Figure 10b). Lower likelihood of ashfall in Auckland unless and until the low system moves off to the east.

Type 2 (T: 12.3%, more common in winter and spring): Dominantly moderate to strong W to NW wind that distributes ash over the eastern North Island towards Hawkes Bay and East Cape with the majority of the ash being carried out over the Pacific Ocean (Figure 4d-f). Very low probability of ashfall in Auckland or Wellington (Figure 10).

Type 3 (SW: 11.3%, no large seasonal control, slightly more common in winter): Strong dominant W wind, may change slightly to NW or SW. Distributes ash towards the Hawkes Bay, East Cape and Bay of Plenty with the majority of the ash being carried out over the Pacific Ocean. Thin ash deposition may occur in Auckland, very low likelihood in Wellington (Figure 10).

Type 4 (NE: 6.3%, more common in summer): Dominant light to moderate N winds, may swing NW or NE, depending on position of low pressure to the west. Ashfall mostly occurs in Hawkes Bay, Wairarapa and lower North Island and may occur in Taranaki during NE winds. Thicker ash deposits are more likely in Wellington for this classification, but very low probability in Auckland (Figure 10).

Type 5 (R: 4.7%, more dominant in summer/autumn): Light to moderate W to SW winds resulting in more spherical distribution over the central and eastern North Island. Thickest ash deposits occur in Hawkes Bay and Bay of Plenty regions, including Tauranga. Thin ash deposits may occur in Auckland, but have a low likelihood in Wellington (Figure 10).

Type 6 (HW: 5.4%, more dominant in summer/autumn): Winds dominantly light to moderate W or SW with ashfall occurring mostly in Hawkes Bay and Bay of Plenty regions.

Thin ash deposition may occur in Auckland at a low probability, but not in Wellington (Figure 10).

Type 7 (HE: 7.1%, no seasonal control): Dominantly light W winds, that may swing to N or S depending on the exact position of the high pressure system to the east. Generate thick deposits in Hawkes Bay and Bay of Plenty. Very low likelihood of ash deposition in Auckland or Wellington (Figure 10).

Type 8 (W: 4.8%, more common in spring): Moderate to strong W winds. Ashfall occurs mostly in Hawkes Bay to East Cape regions with the majority of the ash being carried out over the Pacific Ocean. Very low likelihood of ashfall in Auckland or Wellington (Figure 10).

Type 9 (HNW: 6.9%, less common in summer): Moderate SW winds deposits ash mostly in East Cape, Bay of Plenty regions. May push ash towards Auckland if high pressure system moves closer to New Zealand (Figure 3, 10a). Very low likelihoood of ashfall in Wellington or the western North Island (Figure 10b).

Type 10 (TNW: 7.6%, no seasonal control): Quite variable winds with either W to SW winds of moderate strength distributing ash over East Cape, or NW winds pushing ash to the Wairarapa/Hawkes Bay regions. Small likelihood of ashfall in Wellington and no ashfall in Auckland (Figure 10).

Type 11 (HSE: 13.7%, significantly more common in summer and autumn). Mostly light winds with minor N,W or S component. Ash widely distributed over North Island, but sensitive to wind direction for smaller sized eruptions (Figure 4a-c). Thick deposits around the central North Island as little ash is blown offshore. High likelihood of thicker deposits in both Auckland and Wellington.

Type 12 (H: 12.9%, less common in summer): Mostly light winds with minor W to S direction, depending on exact position of high pressure system (Figure 3). Thick deposits around the central North Island, especially towards East Cape and Bay of Plenty as little ash is blown offshore. High likelihood of thicker deposits in both Auckland in S winds, but lower likelihood in Wellington (Figure 10).

Conclusions and key findings

This EQC-funded research project has investigated ashfall hazards from future potential explosive eruptions from Taupo volcano and found that:

1. A wide range of eruption sizes are possible given the geological and magmatic history of Taupo. Future explosive events are most likely to be ~0.1 km^3 in volume but could range up to 500 km^3 in the maximum credible event, but at very low overall probability of occurrence. Probabilistic hazard models such as those used for earthquakes have been successfully applied to volcanoes like Taupo (e.g. *Hurst and Smith*, 2004, 2010) in order to estimate return periods for ashfall at specific locations for risk management purposes. However, our scenario-based approach to hazard modeling captures the variability of ash dispersal with increasing eruption size and diverse weather conditions and highlights their variable roles.

2. Simulations of ashfall using the dispersal model Ash3d (*Schwaiger et al*., 2012) show a wide range of outputs. On an individual basis, each model simulation and the resulting ash deposit maps are highly sensitive to the start time of the eruption and the wide range of possible wind conditions. There is no strong seasonal variability in ash dispersal but final deposit maps generally conform with the synoptic-climatological classifications of *Kidson* (2000) which describes 12 main weather regimes that occur in New Zealand.

3. With increasing eruption size, the formation of an umbrella cloud may push significant amounts of ash upwind and crosswind as the plume becomes less sensitive to the weather conditions due to the increasing role of density-driven dispersal in the plume. However, strong stratospheric winds may still play a major role in controlling medium- to long-range dispersal and which particular areas of New Zealand receive significant levels of ashfall. The strength of the umbrella cloud may also greatly affect the amount of time it takes for ash to start falling at major towns or cities, by a factor of up to 200%.

4. Probability maps produced from 1000 dispersal simulations highlight the dominance of westerly winds across the central North Island, with regions in the central and eastern North Island having the highest probability of significant ashfall. The shape of probability contours becomes more circular with increasing eruption size, reflecting the increasing role of the umbrella cloud in controlling the dispersal of ash in the plume. For smaller eruptions (0.1 km^3), ashfall thickness at major towns

around the North Island are typically <10 mm. However, with increasing sizes, the probability of ash thickness to reach damaging levels (10-100 mm) becomes significant, especially in the Gisborne, Hawke's Bay, Bay of Plenty, Waikato and Manawatu regions. For the largest eruptions (50-500 km^3), major damage (100mm) or severe structural damage (>300 mm) can be expected at high probabilities in most major towns or cities in the North Island, even as far away as Auckland or Wellington. Ashfall >1 cm in thickness will also occur in the South Island for these large eruptions at significant probabilities.

5. Particular wind conditions result in increased probabilities of ashfall in different locations around New Zealand, highlighting the dependence of ashfall hazards from Taupo eruptions on weather. In general, synoptic weather classifications (Kidson types) associated with light winds such as those experienced during zonal or blocking regimes result in the thickest ashfall at major towns and cities. Particular Kidson types associated with ashfall in distal locations like Auckland and Wellington are the HSE (type 11) and H (type 12) types (on average occurring about one-quarter of the time) where a large high pressure system is situated close to or over the North Island. Apart from the TSW Kidson type, trough regimes and strong associated westerly winds lead to most of the ash being distributed off to the east and over the Pacific Ocean, resulting in the least amount of ashfall at most major towns or cities.

6. Understanding ashfall hazards at caldera volcanoes like Taupo is inherently difficult, because of the wide range in possible eruption sizes. Our approach, however, has revealed the key parameters controlling ash dispersal from events ranging over several orders of magnitude. We have thus been able to highlight which particular areas of New Zealand are vulnerable to ashfall under different conditions from future potential Taupo eruptions. Our scenario-based probabilistic approach incorporating diverse eruptive sizes may prove useful at other caldera volcanoes globally and opens up new avenues for future eruption planning, hazard management and ongoing risk studies.

Impact

Our research has demonstrated the wide range of ash thicknesses that may occur at major population centres around New Zealand from future explosive eruptions of Taupo volcano and the conditions under which potentially damaging amounts of ash may accumulate. This information is crucial for hazard planning, risk management and for assessing critical

infrastructure and areas of vulnerability, particularly in regions in the central and eastern North Island, which have high probabilities of ashfall, even in smaller events. The results from this study will form the basis of ongoing risk studies to calculate the areas of highest risk and how impact can be reduced my improving infrastructure and disaster management plans which will be shared with Civil Defense and local council hazard teams. We envisage that the results of our work will also be used in future emergency management and risk-management planning exercises and programmes.

Future work

The results of this study, mostly in the form of ash thickness-probability maps, will be used in future risk studies to estimate potential costs of future Taupo eruptions to the New Zealand economy and to investigate areas of vulnerability in towns where heavy ashfall can be expected (e.g. Gisborne/Napier). This work will be done in collaboration with key risk researchers at University of Canterbury (Tom Wilson) and GNS (Natalia Deligne). Future ashfall modeling and refinement of eruption scenarios will continue and be funded in part by the MBIE-funded ECLIPSE (Eruption or Catastrophe: Learning to Implement Preparedness for future Supervolcano Eruptions) project. This $8.2 million programme will create world-class scientific knowledge that will inform and enable Iwi and Civil Defence to deal with the likelihood and impact of future events, whether unrest or eruption. Future work based on the results of this EQC study will help assess what the impacts are of future Taupo eruptions and how to best support emergency management decision making.

Acknowledgements

We thank Richard Smith and Priscilla Cheng from EQC for their support of this research project, for attending our ashfall workshop and for helpful feedback and suggestions. Hans Schwaiger from the USGS assisted with technical issues with Ash3d. SB would like to thank the USGS for hosting him during visits to the Cascades Volcano Observatory. Heather Wright, John Pallister and Carl Thornber from the USGS, Graham Leonard, Tony Hurst and Natalia Deligne from GNS and Iman Soltanzadeh from MetService also provided helpful suggestions and discussions during this work.

References

Allan, A. S. R., Wilson, C. J. N., Millet, M-A. & Wysoczanski, R. J. (2012). The invisible hand: tectonic triggering and modulation of a rhyolitic supereruption. *Geology*, *40*(6), 563–566. https://doi.org/10.1130/G32969.1.

Aramaki, S. (1984). Formation of the Aira Caldera, southern Kyushu, ~22,000 years ago. *Journal of Geophysical Research*, *89*(B10), 8485–8501. https://doi.org/10.1029/JB089iB10p08485

Barker, S. J., Wilson, C. J. N., Allan, A. S. R., & Schipper, C. I. (2015). Fine-scale temporal recovery, reconstruction and evolution of a post-supereruption magma system. *Contributions to Mineralogy and Petrology*, *170*(1), 5. https://doi.org/10.1007/s00410-015-1155-2

Barker, S. J., Wilson, C. J. N., Morgan, D. J., & Rowland, J. V. (2016). Rapid priming, accumulation and recharge of magma driving recent eruptions at a hyperactive caldera volcano. *Geology*, *44*(4), 323–326. https://doi.org/10.1130/G37382.1

Blong, R. J. (1984). *Volcanic hazards: a sourcebook on the effects of eruptions.* North Ryde, N.S.W: Academic Press Australia.

Carey, S., & Sigurdsson, H. (1989). The intensity of Plinian eruptions. *Bulletin of Volcanology*, *51*(1), 28–40. https://doi.org/10.1007/BF01086759

Carey, S. N., & Sparks R. S. J. (1986). Quantitative models of the fallout and dispersal of tephra from volcanic eruption columns. *Bulletin of Volcanology*, *48*(2-3), 109–125. https://doi.org/10.1007/BF01046546

Christiansen, R. L. (2001). The Quaternary and Pliocene Yellowstone Plateau volcanic field of Wyoming, Idaho, and Montana. *U. S. Geological Survey Professional Paper 729-G.* Washington, D.C.: United States Government Printing Office.

Costa, A., Dell'Erba, F. Di Vito, M. A. , Isaia, R., Macedonio, G., Orsi, G., & Pfeiffer, T. (2009). Tephra fallout hazard assessment at the Campi Flegrei caldera (Italy). *Bulletin of Volcanology*, 71, 259–273. https://doi.org/10.1007/s00445-008-0220-3

Cronin, S. J., Hedley, M. J., Neal, V. E., & Smith, R. G. (1998). Agronomic impact of tephra fallout from the 1995 and 1996 Ruapehu Volcano eruptions, New Zealand. *Environmental Geology, 34*(1), 21–30. https://doi.org/10.1007/s002540050253

Davies, T., Beaven, S. , Conradson, D., Densmore, A., Gaillard, J. C., Johnston, D., et al. (2015). Towards disaster resilience: A scenario-based approach to co-producing and integrating hazard and risk knowledge. *International Journal of Disaster Risk Reduction,* 13, 242–247. https://doi.org/10.1016/j.ijdrr.2015.05.009

De Natale, G., Troise, C., Kilburn, C. R. J., Somma, R., & Moretti, R. (2017). Understanding volcanic hazard at the most populated caldera in the world: Campi Flegrei, Southern Italy. *Geochemistry, Geophysics, Geosyst*ems, *18*(5), 2004–2008. https://doi.org/10.1002/2017GC006972

Di Vito, M. A., Isaia, R., Orsi, G., Southon, J., de Vita, S., D'Antonio, M. D., et al. (1999). Volcanism and deformation since 12,000 years at the Campi Flegrei caldera (Italy). *Journal of Volcanology and Geothermal Research*, *91*(2-4), 221–246. https://doi.org/10.1016/S0377-0273(99)00037-2

Dominy-Howes, D., & Minos-Minopoulos, D. (2004). Perceptions of hazard and risk on Santorini. *Journal of Volcanology and Geothermal Research, 137*(4), 285–310. https://doi.org/10.1016/j.jvolgeores.2004.06.002

Druitt, T. H., Edwards, L., Mellors, R. M., Pyle, D. M., Sparks, R. S. J., Lanphere, M., et al. (1999). Santorini Volcano*. Geological Society Memoirs,* 19. Geological Society, London. https://doi.org/10.1144/GSL.MEM.1999.019.01.12

Durant, A. J., Rose, W. I., Sarna-Wojcicki, A. M., Carey, S., & Volentik, A.C. (2009). Hydrometeor-enhanced tephra sedimentation: Constraints from the 18 May 1980 eruption of Mount St. Helens (USA). *Journal of Geophysical Research,* 114, B03204. https://doi.org/10.1029/2008JB005756.

Hildreth, W. (2004). Volcanological perspectives on Long Valley, Mammoth Mountain, and Mono Craters: several contiguous but discrete systems. *Journal of Volcanology and Geothermal Research, 136*(3-4), 169–198. https://doi.org/10.1016/j.jvolgeores.2004.05.019

Hill, D. P., & Prejean, S. (2005). Magmatic unrest beneath Mammoth Mountain, California. *Journal of Volcanology and Geothermal Research*, *67*(4), 8–15. https://doi.org/10.1016/j.jvolgeores.2005.03.002

Hogg, A. G., Lowe, D. J., Palmer, J., Boswijk, G., & Bronk Ramsey C. (2012). Revised calendar date for the Taupo eruption derived by ^{14}C wiggle-matching using a New Zealand kauri ^{14}C calibration data set. *Holocene*, *22*(4), 439–449. https://doi.org/10.1177/0959683611425551

Houghton, B. F., Carey, R. J., Cashman, K. V., Wilson, C. J. N., Hobden, B. J., & Hammer, J. E. (2010). Diverse patterns of ascent, degassing, and eruption of rhyolite magma during the 1.8 ka Taupo eruption, New Zealand: evidence from clast vesicularity. *Journal of Volcanology and Geothermal Research, 195*(1), 31–47. https://doi.org/10.1016/j.jvolgeores.2010.06.002

Hurst, T., & Smith, W. (2004). A Monte Carlo methodology for modelling ashfall hazards. *Journal of Volcanology and Geothermal Research, 138*(3-4), 393–403. https://doi.org/10.1016/j.jvolgeores.2004.08.001

Hurst, T., & Smith, W. (2010). Volcanic ashfall in New Zealand - probabilistic hazard modelling from multiple sources. *New Zealand Journal of Geology and Geophysics*, *53*(1), 1–14. https://doi.org/10.1080/00288301003631129

Jenkins, S. F., Wilson, T. M., Magill, C. R., Miller, V., Stewart, C., Blong, R., et al. (2015). Volcanic ash fall hazard and risk. In S.C. Loughlin, R.S.J. Sparks, S.K. Brown, S.F. Jenkins and C. Vye-Brown (Eds.), *Global volcanic hazards and risk* (pp. 173–222). Cambridge: Cambridge University Press. https://doi.org/10.1017/CBO9781316276273

Jiang, N., Hay, J. E., & Fisher G.W. (2004). Classification of New Zealand synoptic weather types and relation to the Southern Oscillation Index. *Weather and Climate*, 23, 3–23.

Johnston, D. M., Houghton, B. F., Neall, V. E., Ronan, K.R., & Paton, D. (2000). Impacts of the 1945 and 1995–1996 Ruapehu eruptions, New Zealand: An example of increasing societal vulnerability. *Geological Society of America Bulletin*, *112*(5), 720–726. https://doi.org/10.1130/0016-7606(2000)112<0720:IOTARE>2.3.CO;2

Kalnay, E., Kanamitsu, M., Kistler, R., Collins, W., Deaven, D., Gandin, L., et al. (1996). The NCEP/NCAR 40-Year Reanalysis Project. *Bulletin of the American Meteorological Society*, *77*(3), 437–471. https://doi.org/10.1175/1520-0477(1996)077<0437:TNYRP>2.0.CO;2

Kidson, J. W. (2000). An analysis of New Zealand synoptic types and their use in defining weather regimes, *International Journal of Climatology*, 20, 299–316. https://doi.org/10.1002/(SICI)1097-0088(20000315)20:3<299::AID-JOC474>3.0.CO;2-B

Langmann, B., Folch, A., Hensch, M., & Matthias, V. (2012). Volcanic ash over Europe during the eruption of Eyjafjallajökull on Iceland, April–May 2010. *Atmospheric Environment,* 48, 1–8. https://doi.org/10.1016/j.atmosenv.2011.03.054

Lowenstern, J. B., Smith, R. B., & Hill, D. P. (2006). Monitoring super-volcanoes: Geophysical and geochemical signals at Yellowstone and other large caldera systems. *Philosophical Transactions of the Royal Society of London, Series A, 364*(1845), 2055–2072. https://doi.org/10.1098/rsta.2006.1813

Mason, B. G., Pyle, D. M., & Oppenheimer, C. (2004). The size and frequency of the largest eruptions on Earth. *Bulletin of Volcanology, 66*(8), 735–748. https://doi.org/10.1007/s00445-004-0355-9

Mastin, L. G., Guffanti, M., Servranckx, R., Webley, P., Barsotti, S., et al. (2009). A multidisciplinary effort to assign realistic source parameters to models of volcanic ash-cloud transport and dispersion during eruptions. *Journal of Volcanology and Geothermal Research*, *186*(1-2), 10–21. doi:10.1016/j.jvolgeores.2009.01.008.

Mastin, L. G., Van Eaton, A. R., & Lowenstern, J. B. (2014). Modeling ash fall distribution from a Yellowstone supereruption. *Geochemistry, Geophysics, Geosyst*ems, *15*(8), 3459-3475. https://doi.org/10.1002/2014GC005469

Mastin, L. G., Van Eaton, A. R., & Durant, A. J. (2016). Adjusting particle-size distributions to account for aggregation in tephra-deposit model forecasts. *Atmospheric Chemistry and Physics,* 16, 9399-9420. https://doi.org/10.5194/acp-16-9399-2016

Oppenheimer, C. (2003). Climatic, environmental and human consequences of the largest known historic eruption: Tambora volcano (Indonesia) 1815. *Progress in Physical Geography*, *27*(2), 230–259. https://doi.org/10.1191/0309133303pp379ra

Potter, S. H., Scott, B. J., Jolly, G. E., Johnston, D. M., & Neall, V. E. (2015). A catalogue of caldera unrest at Taupo Volcanic Centre, New Zealand, using the Volcanic Unrest Index (VUI). *Bulletin of Volcanology,* 77(9), 78. https://doi.org/10.1007/s00445-015-0956-5

Renwick, J. A. (2011). Kidson's synoptic weather types and surface climate variability over New Zealand. *Weather and Climate*, 31, 3–32.

Rhoades D. A., Dowrick, D. J., & Wilson, C. J. N. (2002). Volcanic hazards in New Zealand: Scaling and attenuation relations for tephra fall deposits from Taupo volcano. *Natural Hazards*, *26*(2), 147-174. https://doi.org/10.1023/A:1015608732356

Rowland, J. V., Wilson, C. J. N., & Gravley, D. M. (2010). Spatial and temporal variations in magma-assisted rifting, Taupo Volcanic Zone, New Zealand. *Journal of Volcanology and Geothermal Research 190*(1-2), 89-108. https://doi.org/10.1016/j.jvolgeores.2009.05.004

Schwaiger, H., Denlinger, R., & Mastin, L. G. (2012). Ash3d: A finite-volume, conservative numerical model for ash transport and tephra deposition. *Journal of Geophysical Research*, 117, B04204. https://doi.org/10.1029/2011JB008968

Self, S. (2006). The effects and consequences of very large explosive volcanic eruptions. *Philosophical Transactions of the Royal Society of London, Series A, 364*(1845), 2073–2097. https://doi.org/10.1098/rsta.2006.1814

Self, S., Rampino, M. R., Newton, M. S., & Wolff, J. A. (1984). Volcanological study of the great Tambora eruption of 1815. *Geology*, *12*(11), 659–663. https://doi.org/10.1130/0091-7613(1984)12<659:VSOTGT>2.0.CO;2

Sigurdsson, H., & Carey, S. (1989). Plinian and co-ignimbrite tephra fall from the 1815 eruption of Tambora volcano. *Bulletin of Volcanology, 51*(4), 243–270. https://doi.org/10.1007/BF01073515

Smith, E. G. C., Williams, T. D., & Darby, D. J. (2007). Principal component analysis and modeling of the subsidence of the shoreline of Lake Taupo, New Zealand, 1983–1999: Evidence for dewatering of a magmatic intrusion? *Journal of Geophysical Research*, 112, B08406. https://doi.org/10.1029/2006JB004652

Stirling, M. W., & Wilson, C. J. N. (2002). Development of a volcanic hazard model for New Zealand: First approaches from the methods of seismic hazard analysis. *Bulletin for the New Zealand Society of Earthquake Engineering*, 35, 266–277.

Thompson, M. A., Lindsay, J. M., Sandri, L., Biass, S., Bonadonna, C., Jolly, G., & Marzocchi, W. (2015). Exploring the influence of vent location and eruption style on tephra fall hazard from the Okataina Volcanic Centre, New Zealand. *Bulletin of Volcanology*, 77, 38. https://doi.org/10.1007/s00445-015-0926-y

Van Eaton, A. R, Herzog, M., Wilson, C. J. N., & McGregor, J. (2012). Ascent dynamics of large phreatomagmatic eruption clouds: the role of microphysics. *Journal of Geophysical Research*, 117, B03203. https://doi.org/10.1029/2011JB008892

Vandergoes, M. J., Hogg, A. G., Lowe, D. J., Newnham, R. M., Denton, G. H., Southon, J., et al. (2013). A revised age for the Kawakawa/Oruanui Tephra, a key marker for the last Glacial Maximum in New Zealand. *Quaternary Science Reviews*, 74, 195-201. https://doi.org/10.1016/j.quascirev.2012.11.006

Walker, G. P. L. (1980). The Taupo Pumice: product of the most powerful known (ultraplinian) eruption? *Journal of Volcanology and Geothermal Research, 8*(1), 69-94. https://doi.org/10.1016/0377-0273(80)90008-6

Wilson, C. J. N. (1993). Stratigraphy, chronology, styles and dynamics of late Quaternary eruptions from Taupo volcano, New Zealand. *Philosophical Transactions of the Royal Society of London, Series A*, *343*(1668), 205-306. https://doi.org/10.1098/rsta.1993.0050

Wilson, C. J. N. (2001). The 26.5 ka Oruanui eruption, New Zealand: an introduction and overview. *Journal of Volcanology and Geothermal Research, 112*(1-4), 133-174. https://doi.org/10.1016/S0377-0273(01)00239-6

Wilson, C. J. N., & Hildreth, W. (1997). The Bishop Tuff: New insights from eruptive stratigraphy. *Journal of Geology*, *105*(4), 407–439. https://doi.org/10.1086/515937

Wilson, C. J. N., & Walker, G. P. L. (1985). The Taupo eruption, New Zealand I. General aspects. *Philosophical Transactions of the Royal Society of London, Series A, 314*(1529), 199-228. https://doi.org/10.1098/rsta.1985.0019

Wilson, C. J. N, Gravley, D. M., Leonard, G. S., Rowland, J. V. (2009). Volcanism in the central Taupo Volcanic Zone, New Zealand: tempo, styles and controls. In: T. Thordarson, S. Self, G. Larsen, S.K. Rowland, A. Hoskuldsson (Eds.), *Studies in Volcanology: The Legacy of George Walker*. London: Geological Society. Special publications of the International Association of Volcanology and Chemistry of the Earth's Interior 2, 225-247.

Wilson, L., & Huang, T. C. (1979). The influence of shape on the atmospheric settling velocity of volcanic ash particles. *Earth and Planetary Science Letters*, *44*(2), 311–324. https://doi.org/10.1016/0012-821X(79)90179-1

Wilson, T. M., Stewart, C., Sword-Daniels, V., Leonard, G. S., Johnston, D. M., Cole, J. W., et al. (2012). Volcanic ash impacts on critical infrastructure. *Physics and Chemistry of the Earth,* 45-46, 5-23. https://doi.org/10.1016/j.pce.2011.06.006

Outputs and Dissemination (and links if possible)

A manuscript based on all the information presented above is currently in preparation to submit to *Journal of Geophysical Research* (https://agupubs.onlinelibrary.wiley.com/journal/21562202)

List of key end users

GNS Science and GeoNet
Civil Defence and Emergency Management (CDEM)
EQC
Regional and District Councils throughout the North Island
Caldera Advisory Group (run through Waikato Regional Council)
Central Plateau Volcanic Advisory Group (run through Ruapehu District Council)
Volcanic Ash Advisory Commission (run through Wellington Meteorological office)
Iwi (Tuwharetoa and Te Arawa in the near-vent area)